Proceedings of 2nd Micro/Nanoscale Heat & Mass Transfer International Conference
MNHMT2009
December 18-21, 2009, Shanghai, China

MNHMT2009-18040

LIQUID-VAPOR OSCILLATING FLOW AND HEAT TRANSFER IN A U-SHAPED MINICHANNEL WITH INTERNAL WICK STRUCTURE

Jiajun Xu, Yuwen Zhang[1,2], and H. B. Ma[2]
Department of Mechanical and Aerospace Engineering
University of Missouri
Columbia, MO 65211, USA

ABSTRACT

Liquid-vapor oscillating flow and heat transfer in a vertically placed oscillating heat pipe (OHP) with a sintered particle wick structure inside are analyzed in this paper. The evaporation and condensation heat transfer coefficients are obtained by solving the microfilm evaporation and condensation on the sintered particles. The sensible heat transfer between the liquid slug and the channel wall are obtained by analytical solution or empirical correlations, depending on whether the liquid flow is laminar or turbulent. The effects of the maximum evaporation and condensation angles on the oscillatory flow, as well as sensible and latent heat transfer are analyzed.

INTRODUCTION

Oscillating Heat Pipe (OHP) is made up of a long, continuous capillary tube bent into many turns, with sufficiently small inner diameter to ensure the formation of liquid slugs. It is as a very promising heat transfer device that can be utilized to transfer a large amount of heat from heating to cooling sections [1]. In addition to its excellent heat transfer capability, it also posses advantages over the conventional heat pipe that include its simple structure and absence of cross-talk between liquid and vapor phases.

Due to the oscillation of the working fluid in the axial direction of the tube, heat is transported from the evaporator section to the condenser section by the liquid slugs via sensible heat, which is dominant when the flow pattern in the OHP is slug flow [2]. Wong et al. [3] proposed a theoretical model of OHP based on a Lagrange approach in which the flow was modeled under adiabatic condition. Hosoda et al. [4] reported a simplified numerical model of a OHP, in which temperature and pressures are calculated by solving the momentum and energy equations for two-dimensional two-phase flow. Shafii et al. [2] developed a theoretical model to simulate the behaviour of liquid slugs and vapor plugs in both closed- and open-loop OHPs with two turns. They concluded that the number of vapor plugs was reduced to the number of heating section no matter how many vapor slugs were initially in the OHP. Therefore, the OHP with even turns is symmetric and can be modelled as several U-shaped channels. Zhang et al. [5] analyzed the liquid-vapor oscillating flow in a U-shaped miniature channel. Xu and Zhang [6] studied sensible and latent heat transfer during liquid-vapor flow in a U-Shaped miniature tube.

Wick structure is commonly used in conventional heat pipes to provide capillary force to return the liquid from condenser section to the evaporator section [7]. Based on the experience in conventional heat pipes, it will be logical to assume that the heat transfer performance an OHP will be improved by adding wick structures. Holly and Faghri [8] analyzed the OHP with capillary wick and built a model to calculate the contribution of adding a sintered particle wick structure. Empirical correlation was used in their work to obtain boiling heat transfer coefficient from the surface of the wick structure. In this paper, liquid-vapor flow and heat transfer in a miniature U-shaped miniature channel will be analyzed.

NOMENCLATURE

A	area, m^2
c_p	specific heat at constant pressure, J/kg-K
c_v	specific heat at constant volume, J/kg-K
d	diameter of the miniature channel, m
h_c	condensation heat transfer coefficient, W/m^2-K
h_e	evaporation heat transfer coefficient, W/m^2-K

[1] Corresponding author. Fellow ASME. Email: zhangyu@missouri.edu
[2] Professor

h_{lv} latent heat, J/kg
k thermal conductivity, W/m
K curvature of meniscus, 1/m
L length, m
m mass of vapor plugs, kg
N number of the thin film
p_d disjoining pressure, N/m^2
r curvature radius of the meniscus, m
p vapor pressure, Pa
$q_{p,con}$ condensation heat transfer on a single particle, W
$q_{p,eva}$ evaporation heat transfer on a single particle, W
$Q_{con,p}$ total condensation heat transfer, W
$Q_{eva,p}$ total evaporation heat transfer, W
$Q_{in,s,l}$ sensible heat transfer into the liquid slug, W
$Q_{out,s,l}$ sensible heat transfer from the liquid slug, W
R gas constant, J/kg K
t time, s
T temperature, K
x_p displacement of the liquid slug, m
Z velocity of the liquid slug, m/s

Greek symbols

α thermal diffusivity, m^2/s
β contact angle, degree
δ film thickness, m
ε porosity
γ ratio of specific heat
ν kinematic viscosity, m^2/s
ρ density, kg/m^3
σ surface tension, N/m
τ_p shear stress, N/m^2

Subscripts

0 initial condition
1 left vapor plug
2 right vapor plug
c condenser
e evaporator
l liquid
p plug
v vapor
w the wall of the tube

Physical Model for Oscillatory Flow

Figure 1 shows a schematic diagram of the physical model. The inner surface of a closed-end U-shaped miniature channel is coated with a layer of sintered metal particles. The inner diameter of the miniature tube measured from the surface of the sintered wick is d and its total length is $2L$. The two heating sections have a length of L_e locating near the two ends of the tube. The middle part between the two heating sections is the cooling section with a length of $2L_c$. The wall temperatures at the heating and cooling sections are T_e and T_c, respectively. The length of the liquid slug is L_p and the displacement of the liquid slug is represented by x_p, which is zero when the liquid slug is exactly in the middle of the U-shaped minichannel.

The displacement of liquid slug can be expressed as [2]:

$$A_c L_p \rho_l \frac{d^2 x_p}{dt^2} = (p_{v1} - p_{v2}) A_c - 2\rho_l g A_c x_p - \pi d L_p \tau_p \qquad (1)$$

where $A_c = \pi d^2/4$ is the cross-sectional area of the tube, $\tau_p = C_l \rho v^2/2$ is the shear stress acting between the liquid slug and the tube. The friction coefficient, C_l, can be determined based on Reynolds number.

Utilizing the first law of thermodynamics to the two vapor plugs and assuming vapor behaviours like ideal gas, the masses and temperatures of the two vapor plugs can be obtained as [5]

$$m_{v1} = \frac{\pi d^2 p_0}{4RT_0}\left(\frac{p_{v1}}{p_0}\right)^{1/\gamma}(L_e + x_p) \qquad (2)$$

$$m_{v2} = \frac{\pi d^2 p_0}{4RT_0}\left(\frac{p_{v2}}{p_0}\right)^{1/\gamma}(L_e - x_p) \qquad (3)$$

$$T_{v1} = T_0\left(\frac{p_{v1}}{p_0}\right)^{(\gamma-1)/\gamma} \qquad (4)$$

$$T_{v2} = T_0\left(\frac{p_{v2}}{p_0}\right)^{(\gamma-1)/\gamma} \qquad (5)$$

The masses of the vapor plugs are related to evaporation and condensation:

$$\frac{dm_{v1}}{dt} = \begin{cases} -h_c \pi d x_p (T_{v1} - T_c)/h_{fg}, & x_p > 0 \\ -h_e \pi d (L_e + x_p)(T_e - T_{v1})/h_{fg}, & x_p < 0 \end{cases} \qquad (6)$$

$$\frac{dm_{v2}}{dt} = \begin{cases} h_e \pi d (L_e - x_p)(T_e - T_{v2})/h_{fg}, & x_p > 0 \\ h_c \pi d x_p (T_{v2} - T_c)/h_{fg}, & x_p < 0 \end{cases} \qquad (7)$$

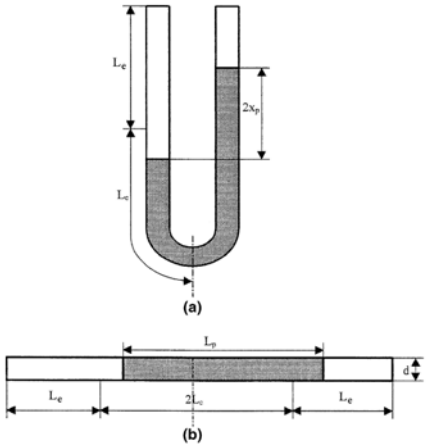

Fig. 1 Physical model

where the heat transfer coefficients in the evaporator and condenser sections, h_e and h_c, must be obtained by solving evaporation and condensation on the top of the sintered particle wick structure.

The reference state of the U-shaped miniature channel is chosen to be the initial state of the system in this work, i.e.

$$x_p = x_{p0}\ ,\ t = 0 \tag{8}$$

$$p_1 = p_2 = p_0\ ,\ t = 0 \tag{9}$$

$$T_1 = T_2 = T_0,\quad t = 0 \tag{10}$$

$$m_{v1} = \frac{\pi d^2 p_0}{4RT_0}(L_e + x_{p0}),\ \ t = 0 \tag{11}$$

$$m_{v2} = \frac{\pi d^2 p_0}{4RT_0}(L_e - x_{p0}),\ \ t = 0 \tag{12}$$

Latent and Sensible Heat Transfer

Evaporation Heat Transfer

For the wick structure located in the heating section, the thin film region can be divided into (1) non-evaporating film, (2) microfilm, and (3) meniscus regions [see Fig. 2(a)]. No evaporation occurs in the non-evaporation thin film region because the liquid-vapor interfacial equilibrium temperature is elevated to the wall temperature due to the disjoining pressure effect. Virtually all of the evaporation occurs in the microfilm region where the disjoining and capillary pressures significantly affect its shape. As the film thickness increases further, the evaporation rate significantly drops, and the curvature stays at a constant value.

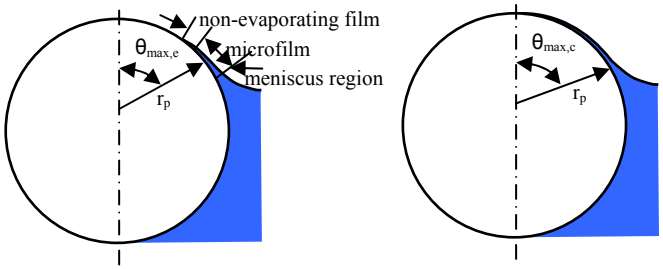

(a) Evaporation model (b) Condensation model

Fig. 2 Evaporation and condensation occurred on sintered particles

Evaporation heat transfer for the case with sintered particle wick is significantly enhanced due to large number of particles. The rate of evaporation heat transfer from a particle can be obtained as [9]

$$q_{p,eva} = 2\pi r_w \sin\theta_{\max,e} k_l (T_e - T_v)\int_0^{10^{-6}} \frac{1}{\delta} dx \tag{13}$$

where $\theta_{\max,e}$ indicates the location of micro region, which was assumed to be π/2 in Ref. [9] but will be treated as a variable in this work. The film thickness can be obtained by analyzing momentum balance with the effect of capillary and disjoining pressure accounted for.

The total evaporating heat transfer may be determined by

$$Q_{eva,p} = N_{p,eva} q_{p,eva} \tag{14}$$

where $N_{p,eva}$ is the total number of particles at the top surface of wicks and it can be found by

$$N_{p,eva} = \frac{(1-\varepsilon)A_{sp}}{\pi r_w^2} = \frac{(1-\varepsilon)\pi dx_{w,eva}}{\pi r_w^2} = \frac{4(1-\varepsilon)dx_{w,eva}}{d_w^2} \tag{15}$$

where $A_{sp} = \pi dx_{w,eva}$ is the total area of top surface of sintered porous medium, ε is the porosity of the sintered wick, and $x_{w,eva}$ is the length of the part expose to evaporation along the tube. The evaporation heat transfer coefficient is

$$h_e = \frac{Q_{p,eva}}{A_{sp}(T_e - T_v)} = \frac{N_{p,eva} q_{p,eva}}{\pi dx_{w,evp}(T_e - T_v)} \tag{16}$$

Condensation Heat Transfer

The physical model of condensation on the sintered wick surface is illustrated in Fig. 2(b). For condensation on a spherical particle in sintered wick, condensation occurs on only part of the sphere (top portion), $\theta < \theta_{max,c}$. The rate of heat transfer for one particle can be obtained by analyzing film condensation for $\theta < \theta_{max,c}$ [10]:

$$q_{p,con} = \frac{\pi}{4} d_w k_\ell (T_{sat} - T_c)\left[\frac{2\mu_\ell k_\ell (T_{sat} - T_c)}{\rho_\ell(\rho_\ell - \rho_v) g h_{\ell v} d_p^3}\right]^{\frac{1}{4}} \cdot \int_0^{\theta_{\max,c}} \sin^{\frac{5}{3}}\theta \left[\int_0^{\theta} \sin^{\frac{5}{3}}\theta d\theta\right] d\theta \tag{17}$$

The number of the sintered particle in the condenser section is:

$$N_{p,con} = \frac{(1-\varepsilon)A_{sp}}{\pi r_w^2} = \frac{(1-\varepsilon)\pi dx_{w,con}}{\pi r_w^2} = \frac{4(1-\varepsilon)dx_{w,con}}{d_w^2} \tag{18}$$

where $x_{w,con}$ is the length of the part expose to condensation along the tube. The total rate heat transfer is the heat transfer rate per particle times the number of particles in the condenser section. Thus, the condensation heat transfer coefficient is

$$h_c = \frac{N_{con,p} q_p}{\pi dx_{w,con}(T_v - T_c)} \tag{19}$$

The sensible heat transfer

The energy equation for the liquid slug in a coordinate system moving with the liquid slug is:

$$\frac{1}{\alpha_l}\frac{\partial T_l}{\partial t} = \frac{\partial^2 T_l}{\partial x_l^2} - \frac{h\pi d}{k_l A}(T_l - T_w) \tag{20}$$

which subjects to the following initial and boundary conditions:

$$T = T_c,\ \ t = 0,\ \ 0 < x_l < L_p \tag{21}$$

$$T = T_{v1},\ \ x_l = 0 \tag{22}$$

$$T = T_{v2},\ \ x_l = L_p \tag{23}$$

The wall temperature of the tube can be either T_e or T_c, depending on the displacement of the liquid slug. The sensible heat transfer into and out from the liquid slug can be obtained

by integrating the heat transfer over the length of the liquid slug [6].

Numerical Solution

Based on the above governing equations and using an implicit scheme, the results of each time-step can be obtained by following the numerical procedure outlined as follows:

1. Assume the temperatures of the two vapor plugs, T_{v1} and T_{v2}
2. Solve for the vapor pressures, p_{v1} and p_{v2}, from eqs. (4) and (5)
3. Solve for x_p from eq. (1).
4. Obtain the new masses of the two vapor plugs, m_{v1}, and m_{v2}, by account for the change of vapor masses from eqs. (6) and (7)
5. Calculate the pressure of the two vapor plugs, p_{v1} and p_{v2}, from eqs. (2) and (3)
6. Solve for T_{v1} and T_{v2} from eqs. (4) and (5)
7. Compare T_{v1} and T_{v2} obtained in step 6 with assumed values in step 1. If the differences meet the small tolerance, then go to the Step 8; otherwise, the above procedure is repeated until a converged solution is obtained.
8. Obtain the evaporation and condensation heat transfer coefficient from eqs. (16) and (19)
9. Solve for liquid temperature distribution from eq. (20) and calculate sensible heat transfer
10. Use eqs. (13) and (17) to calculate latent heat transfer.

After the time-step independent test, it was found that the time-step independent solution of the problem can be obtained when time-step is $\Delta t = 1\times10^{-4}$, which is used in all numerical simulations.

Results and Discussions

The parameters of the U-shaped miniature tube without wick structure are based on those used in Ref. [2]. The parameters of the miniature channel are: L_e = 0.1 m, L_c = 0.185 m, L_p = 0.35, d = 0.0015m, T_e = 120 °C, T_c =20 °C. The initial pressures of the vapor plugs are p_{vi} = 5628 Pa and the initial temperature of the vapor plug is T_{vi} = 35 °C. The heat transfer coefficient at the heating wall is h_h = 150 W/m^2-K and the heat transfer coefficient at the cooling wall is h_c = 100 W/m^2-K. The inner diameters of the U-shaped miniature channels with and without the sintered particles are considered to be the same so that the difference between the two sets of the results are due to the effect of the sintered particles only. The diameter of the sintered particles is d_w = 0.000135m and the porosity of the sintered wick is ε = 0.4. The two angles $\theta_{\max,e}$ and $\theta_{\min,c}$ are set to be equal to be 60°.

Figure 3(a) shows the comparison of the displacement for the cases with and without sintered particles. It can be seen that, after wick is added, the magnitude of the liquid slug displacement is increased by 20% and the phase is slightly delayed. The frequency of oscillation for the cases with sintered particles wick is decreased compared with that of the case without wick. Figure 3(b) shows the comparison of vapor plug temperatures for the cases with and without sintered particle wick. It can be seen that the temperature of left vapor plug with wick has a much wider temperature range: while the maximum temperature is increased by about 5%, the minimum temperature is decreased from around 55°C to about 40°C. Similar to the trend on liquid slug displacement, there is a slight delay in the phase for the case with sintered particle wick, and the frequency is decreased. The variations of the pressures of the left vapor plugs for the cases without and with

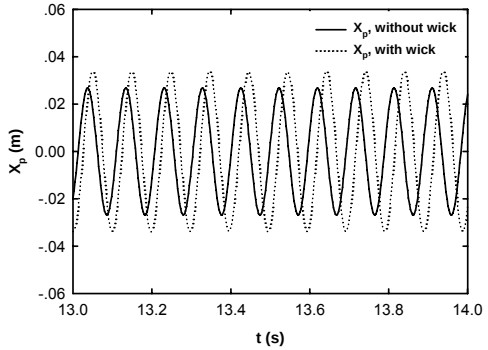

(a) Displacement of liquid slug

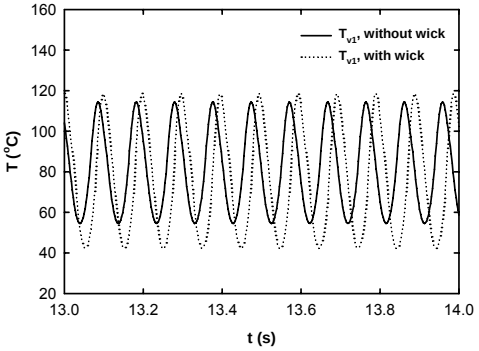

(b) Vapor plug temperatures

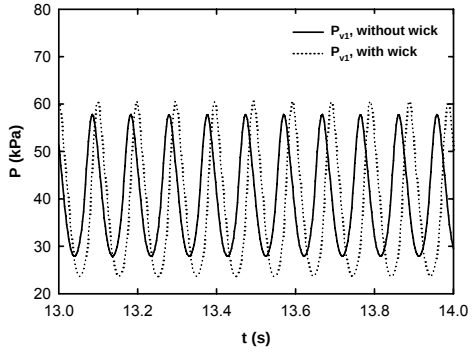

(c) Vapor plug pressure

Fig. 3 Comparison of liquid slug displacement, and temperature and pressure of vapor plugs

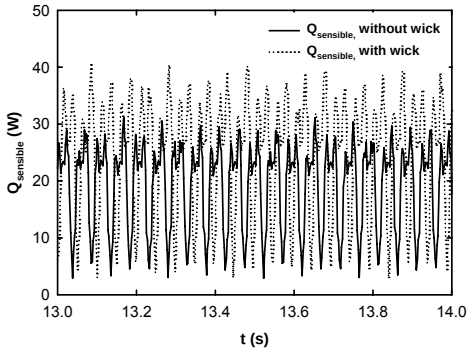

(a) Sensible heat transfer

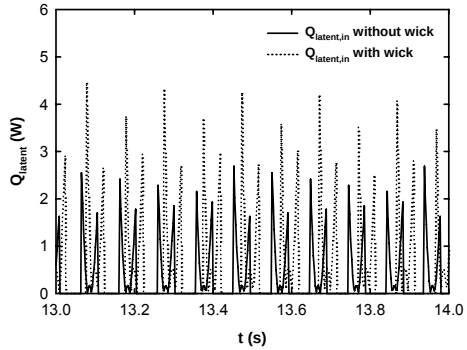

(b) Latent heat transfer

Fig. 4 Comparison of sensible and evaporative heat transfer

wick structure are shown in Fig. 3(c). It can be seen that the addition of sintered particle wick exhibited the similar trend as the vapor plug temperatures. Therefore, one can conclude that adding the wick will increase the amplitudes of displacement, vapor plug temperature and pressure, while the frequency will slightly decrease.

Figure 4(a) shows the comparison of sensible heat transfer transferred into the liquid for the cases with and without wick structure. The phase of the oscillation of sensible heat transfer in and out of the liquid slug is slightly delayed after the addition of the wick. Due to enhanced oscillatory motion of the liquid slug, the average sensible heat transfer rate is increased from 22.39W without sintered particle wick to 26.57W with wick – a 19.1% increase. The comparison of latent heat transfer for the cases with and without wick is shown in Fig. 4(b). It is seen that the evaporation heat transfer is greatly enhanced with addition of the sintered particle wick. Due to the increase of evaporation area and new evaporation mechanism, the average evaporation heat transfer increases from 0.39W to 0.64W – a 90% increase. Thus, the addition of sintered particles changed the evaporation /condensation mechanism in a similar trend as on the other parameters, but with a significantly large magnitude. The overall heat transfer enhancement after addition of wick – including both sensible and latent heat transfer – is about 20%.

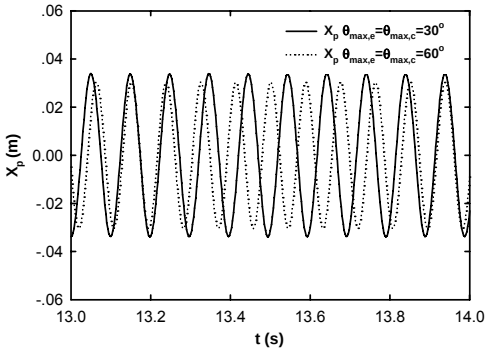

(a) Liquid slug displacement

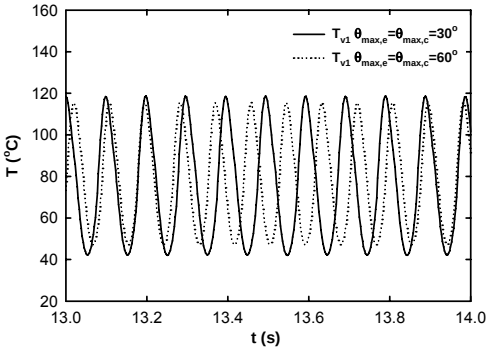

(b) Vapor plug temperature

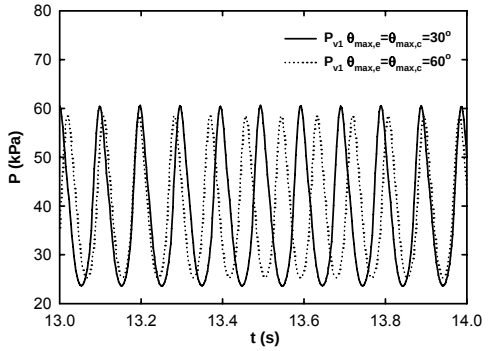

(c) Vapor plug pressures

Fig. 5 Effect of $\theta_{max,e}$ and $\theta_{max,c}$ on the Effect of different heating section temperatures with wick

The effect of the maximum evaporation and condensation angle, $\theta_{max,e}$ and $\theta_{max,c}$ is analyzed and the results are shown in Figs. 5 and 6. As the maximum evaporation and condensation angle decreases from 60° to 30°, the amplitude of displacement is decreased by about 15% while the frequency is increased by about 10%. The temperature and pressure experience a similar decrease as shown in Fig. 5 (b) and (c): the maximum temperature is decreased from around 120°C to 115°C and the minimum temperature is reduced from 40°C to about 45°C, while the maximum pressure is decreased from around 60 kPa to 56 kPa and the minimum value increases from 23 kPa to 25

kPa. Figure 14 shows the effect of the maximum evaporation and condensation angle on sensible and latent heat transfer. It is seen that maximum sensible and latent heat transfer are both decreased while the oscillation curves are still similar. In Fig. 6(a), the maximum sensible heat transfer decrease from around 40W to 38W and the frequency is increased. In Fig. 6(b), the maximum evaporative heat transfer changes from 4.5W to about 3W. The average sensible and latent heat transfer are 24.36 W and 0.61 W, respectively. Therefore, the decrease of $\theta_{max,e}$ and $\theta_{max,c}$ result in decreasing the latent heat transfer but its effect on sensible heat transfer is insignificant.

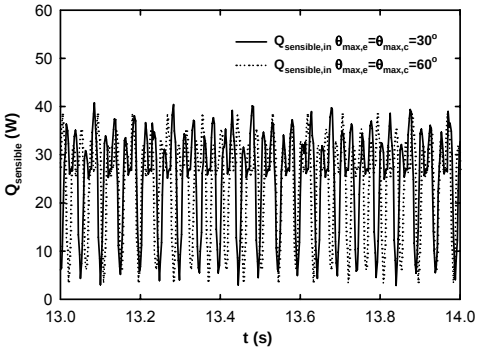

(a) Sensible heat transfer

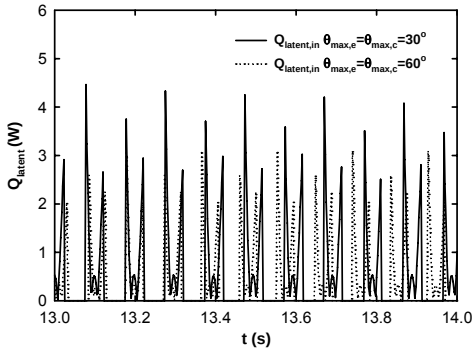

(b) Latent heat transfer

Fig. 6 Effect of $\theta_{max,e}$ and $\theta_{max,c}$ on sensible and evaporative heat transfer with wick

Conclusions

The effect of internal wick structure on the oscillatory flow and heat transfer of an oscillating heat pipe is investigated. The results show that the addition of the wick greatly increases the latent heat transfer as expected and the sensible heat transfer is also increased. The increase of latent heat transfer also causes increases vapor plug temperature and pressure, as well as the amplitude of the liquid slug oscillation. The overall heat transfer is decreased by decreasing maximum evaporation and condensation angle.

Acknowledgement

The work presented in this article was funded by the Office of Naval Research Grant No. N00014-06-1-1119 directed by Dr. Mark Spector.

References

[1] Zhang, Y, and Faghri, A, Advances and Unsolved Issues in Pulsating Heat Pipes, *Heat Transfer Engineering*, Vol. 29, No. 1, pp. 20-44, 2008.

[2] Shafii, M.B., Faghri, A., and Zhang, Y., Thermal Modeling of Unlooped and Looped Pulsating Heat Pipes, ASME Journal of Heat Transfer, Vol. 123, pp. 1159-1171, 2001.

[3] Wong, T.N., Tong, B.Y., Lim, SM., and Ooi, K.T., "Theoretical Modeling of Pulsating Heat Pipe," *Proceedings of the 11th International Heat Pipe Conference,* pp. 159-163, Tokyo, Japan, 1999.

[4] Hosoda, M., Nishio, S., and Shirakashi, R., 1999, "Meandering Closed-Loop Heat-Transfer Tube (Propagation Phenomena of Vapor Plug)," *Proceedings of the 5th ASME/JSME Joint Thermal Engineering Conference*, March 15-19, San Diego, CA

[5] Zhang, Y., Faghri, A., and Shafii. M.B., Analysis of Liquid-Vapor Oscillating Flow in a U-Shaped Miniature Tube, International Journal of Heat and Mass Transfer, Vol. 45, pp. 2501-2508, 2002

[6] Xu, J., and Zhang, Y., Analysis of Heat Transfer during Liquid-Vapor Oscillating Flow in a U-Shaped Miniature Channel, Journal of Enhanced Heat Transfer, 2008 (in press)

[7] Faghri, A., 1995, Heat Pipe Science and Technology, Taylor & Francis, Washington, DC.

[8] Holley, B., and Faghri, A., Analysis of Pulsating Heat Pipe with Capillary Wick and Varying Channel Diameter, International Journal of Heat and Mass Transfer, Vol. 48, pp. 2635-2651, 2005.

[9] M.A, Hanlon,, and H.B, Ma., Evaporation Heat Transfer in Sintered Porous Media, Journal of Heat Transfer, Vol. 125, pp. 644-652, 2003.

[10] Carey, V. P., Liquid-Vapor Phase-Change Phenomena: An Introduction to the Thermophysics of Vaporization and Condensation Processes in Heat Transfer Equipment, Hemisphere Publishing Corp., Washington, D.C., 1992